Available online at www.sciencedirect.com
SCIENCE DIRECT
Polymer 45 (2004) 8531–8540
polymer
www.elsevier.com/locate/polymer

Concentration dependence of static and hydrodynamic screening lengths for three different polymers in a variety of solvents

A. Bennett[a], P.J. Daivis[a,*], R. Shanks[b], R. Knott[c]

[a]CRC for Polymers, Applied Physics, School of Applied Sciences, RMIT University, GPO Box 2476V, Melbourne, Vic. 3001, Australia
[b]CRC for Polymers, Applied Chemistry, School of Applied Sciences, RMIT University, GPO Box 2476V, Melbourne, Vic. 3001, Australia
[c]Australian Nuclear Science and Technology Organization, PMB 1, Menai, NSW 2234, Australia

Received 22 May 2004; received in revised form 9 October 2004; accepted 12 October 2004
Available online 28 October 2004

Abstract

We have used small angle neutron scattering and dynamic light scattering to measure the static and hydrodynamic screening lengths of polystyrene, polymethylmethacrylate and polydimethylsiloxane solutions ranging from marginal to good solvent quality. A universal plot is found for the scaled static screening length when the concentration is scaled using the second virial coefficient in the way suggested by renormalization group theories. The same concentration units do not produce a universal plot for the hydrodynamic screening length at the molecular weights that we have studied (all around $1–2\times10^5$ g/mol). However, when the concentration is expressed in terms of k_Dc, where k_D is the virial expansion coefficient for the cooperative diffusion coefficient and c is the concentration, most of the variation between different polymer–solvent combinations is eliminated. The ratio of hydrodynamic screening length to static screening length increases with concentration for all of the polymer solvent pairs studied, and its value differs for different polymer solvent pairs.

Keywords: Characteristic length; Polymer solution; Static screening length

1. Introduction

The idea of universality has led to the development of a simple, comprehensive and generally successful description of semidilute polymer solution properties for uncharged polymers [1–7]. Universality implies that a single curve should be obtained when a property such as the radius of gyration or osmotic pressure is normalized and then plotted against an appropriately chosen measure of concentration, regardless of specific details of the polymer, solvent and their interaction.

Experimental verification of universality and its theoretical framework of scaling and renormalization-group theory for polymer solutions has proceeded steadily. A comprehensive collection of data displaying universality for a variety of polymer–solvent systems has been presented by Brown and Nicolai [6]. They found that the scaling and renormalization-group theory predictions for the concentration dependence of the static screening length are verified for concentrations large enough for molecular weight independence to be observed, provided that the molecular weight is high enough for a true semidilute region to exist. In addition, they found that the scaling theory prediction for the concentration exponent of the hydrodynamic screening length is verified and the shape of the curve predicted by renormalization-group theory is correct, but the prefactor is underestimated. Although several different solvents are represented in their data collection, all of the solutions considered contained the same polymer–polystyrene.

There are very good reasons for choosing to test theories of polymer solutions using polystyrene. One is that it is commercially available in a well-characterised, monodisperse form. Another is that a large body of reliable work on the properties of polystyrene solutions already exists for comparison. However, the universality hypothesis cannot be truly considered to be verified without considering data obtained for a variety of polymers in a wide range of different solvents. For this reason, Brown and Nicolai [6]

* Corresponding author. Tel.: +61 3 99253393; fax: +61 3 99255290.
E-mail address: peter.daivis@rmit.edu.au (P.J. Daivis).

0032-3861/$ - see front matter © 2004 Elsevier Ltd. All rights reserved.
doi:10.1016/j.polymer.2004.10.018

specifically comment on the need for experimental results for a variety of polymers in addition to polystyrene.

In this paper, we respond to this need by presenting results for the concentration dependence of the static and dynamic screening lengths of polymer solutions obtained from measurements made on polystyrene, polymethylmethacrylate and polydimethylsiloxane in a variety of good and marginal solvents using small angle neutron scattering and dynamic light scattering.

2. Experimental

2.1. Polymers and solvents

The properties of polymers used in our experiments are shown in Table 1. Throughout this paper, polystyrene is abbreviated as PS, deutero-polystyrene as d-PS, polymethylmethacrylate as PMMA and polydimethylsiloxane as PDMS. All of the polymers used were commercially available, relatively monodisperse materials. Of particular interest in Table 1 is the variation in characteristic ratio C_∞ of the three polymers used, polystyrene (PS) being the least flexible and polydimethylsiloxane (PDMS) the most. It is perhaps more relevant to compare the different materials in terms of the number of Kuhn steps per molecule in the unperturbed state. The last column of Table 1 lists the experiments performed on each sample. The properties of solvents used in these experiments are given in Table 2. The names of the solvents are abbreviated as follows: (deuterated) tetrahydrofuran is (d-)THF; (deuterated) toluene is (d-)Tol; deuterated benzene is d-Benz; carbon tetrachloride is CCl_4; and dichloromethane is DCM. All solvents used were spectroscopic grade, obtained either from Aldrich Chemical Co. or Cambridge Isotope Laboratories. The THF was dried with 3 Å molecular sieves and stored in a dessicator to reduce moisture contamination.

The characteristics of solutions studied in these experiments are given in Table 3.

2.2. Small angle neutron scattering

The static screening length was measured by small angle neutron scattering, using the recently developed ANSTO SANS facility at the Australian Nuclear Science and Technology Organisation, Lucas Heights, Australia and the NG-1 beamline of the NIST Centre for Neutron Research, Gaithersberg, USA [8]. The characteristics of the two instruments are summarised in Table 4. The far lower neutron flux of the ANSTO SANS instrument made it necessary to use much greater data acquisition times for this instrument (up to 6 h per sample) than for the NIST NG-1 instrument (up to 60 min per sample). SANS samples were prepared in Spectrosil quartz cells with path lengths ranging from 1 to 5 mm, so as to minimize the effect of multiple scattering. The characteristics of the two SANS beams and detector settings are shown in Table 4. The fundamentals of small angle neutron scattering from polymer solutions are well known [10]. The intensity due to scattering from the sample was obtained from the measured intensity by applying corrections due to background neutron detections and attenuation of the scattered beam by the sample using the measured transmissions of the sample, solvent and empty cell. The resultant total measured intensity due to scattering by the sample is given by

$$I_m(q) = I_I + I_C = I_I + I_0 K \langle b \rangle^2 S(q) \quad (1)$$

where $q = (4\pi/\lambda)\sin(\theta/2)$ is the magnitude of the scattering vector, I_I is the incoherent scattering component, I_C is the coherent scattering component, $S(q)$ is the static structure factor, $\langle b \rangle$ is the effective scattering length of the sample, and K is an instrumental factor. The quantity of interest is the static structure factor, so the incoherent scattering must be either eliminated or accurately estimated during the data analysis step. Polymer solutions for neutron scattering experiments are often made from deuterated polymers in normal solvents, so that the incoherent background scattering is almost exclusively due to ^{1}H nuclei in the solvent, and can be removed by measuring the scattering from a 'blank' sample of pure solvent. This is made possible by the ready availability of deuterated polystyrene, and was the method we used in our experiments on d-PS. Other polymers, such as PMMA and PDMS are far more difficult to obtain in deuterated form. High contrast can be achieved by performing experiments on normal polymers dissolved in deuterated solvents, but performing the experiments in this

Table 1
Polymer properties

Polymer	Source	M_w (g/mol)	M_w/M_n	C_∞	Experiment
PS	Polymer Standards Service	109,000	1.05	10	DLS
d-PS	Polymer Source, Inc.	110,500	1.03	10	SANS[a]
PMMA	Polymer Source, Inc.	202,100	1.11	8.65	SANS[b], DLS
PDMS1	Polymer Source, Inc.	80,500	1.15	6.25	DLS
PDMS2	Polymer Source, Inc.	96,700	1.14	6.25	SANS[c]

[a] At ANSTO.
[b] At ANSTO and NIST.
[c] At ANSTO and NIST.

Table 2
Solvent properties

Solvent	Chemical formula	M (g/mol)	Density (g/ml)	Viscosity (cP) at 25 °C	Refractive Index
d-THF	C_4D_8O	80.157	0.99	0.456	1.4043
d-Tol	C_7D_8	100.191	0.94	0.56	1.494
d-Benz	C_6D_6	84.152	0.948	0.69 at 20 °C	1.4991
CCl_4	CCl_4	153.822	1.594	0.908	1.4601
DCM	CH_2Cl_2	84.932	1.3266	0.413	1.4242
Tol	C_7H_8	92.14	0.861	0.56	1.494
THF	C_4H_8O	72.106	0.8833	0.456	1.405

way makes the ^{1}H incoherent scattering contribution subtraction more difficult. There are two known ways of solving this problem. One is to perform careful incoherent scattering correction, the other is to use neutron polarization analysis to remove the incoherent scattering from the signal. We chose to use the first method, because it could be applied to data collected on the standard SANS beamlines that were available to us. Two independent methods were used to correct for incoherent scattering. We assumed that the incoherent scattering component was correctly estimated from the intensity at very large scattering vector, since it is q-independent. The incoherent scattering component was obtained by fitting an exponential plus a constant to the large-q data. This value for I_I was checked by computing the incoherent scattering cross section for each polymer composition. We found that the estimated incoherent scattered intensity was directly proportional to the calculated incoherent cross section in each case, confirming that our background estimation procedure was valid.

The static structure factor depends on correlations in the positions of the scattering nuclei. For small angle scattering from a semidilute solution of a single polymer species in a solvent, the structure factor can be written as

$$S(q) = \frac{f_{T,c}}{q^2 + \xi_s^{-2}}, \quad (2)$$

where $f_{T,c}$ is a temperature and concentration dependent parameter. The static screening length, ξ_s, was found by fitting a straight line to the linear section of the I_C^{-1} vs q^2 data at each semidilute concentration. The gradient and intercept were determined, and ξ_s^2 and was calculated from their ratio. Uncertainties in values of ξ_s^2 were obtained from the uncertainties in the least squares fitting coefficients.

SANS experiments were performed at a temperature of 23.0 ± 0.5 °C.

Table 3
The experimental concentration and volume fraction ranges for each system

Solution	Experimental technique	Concentration range (mg/ml)	Volume fraction range
d-PS/THF	SANS	20–130	0.016–0.105
PS/THF	DLS	5–100	0.005–0.091
PS/Tol	DLS	5–60	0.005–0.056
PS/CCl_4	DLS	5–125	0.005–0.116
PS/DCM	DLS	5–135	0.005–0.125
PMMA/d-THF	SANS	15–135	0.012–0.109
	DLS	20–95	0.016–0.077
PMMA/THF	DLS	5–100	0.004–0.081
PMMA/d-Tol	SANS	5–115	0.004–0.093
PMMA/d-Benz	SANS	10–140	0.008–0.115
PDMS/d-THF	SANS	10–140	0.010–0.143
PDMS/d-Tol	SANS	10–75	0.010–0.077
	DLS	5–140	0.005–0.143
PDMS/d-Benz	SANS	15–130	0.015–0.133
	DLS	5–160	0.005–0.164

2.3. Dynamic light scattering

Dynamic light scattering (DLS) measurements were performed by measuring the photocount autocorrelation function of light scattered from the polymer solutions using the ALV two-colour cross-correlation multiple scattering suppression spectrometer located at RMIT University. This instrument has been described previously [11]. The spectrometer was operated in single-colour, autocorrelation mode because multiple scattering was negligible, due to the low intensity of light scattered from our polymer solutions. An ALV-5000 Multiple Tau Digital Correlator was used to measure the normalized photocount autocorrelation function of the scattered light, from which the electric field autocorrelation function was obtained.

Samples were prepared by dissolving the polymer in solvent, allowing at least 4 days for dissolution, during which they were periodically agitated, and then filtering directly into scattering cells through 0.2 μm teflon filters on a laminar flow clean bench. All sample phials and scattering cells were flushed with condensing acetone vapour to remove dust, and then thoroughly dried before use. Sample masses were monitored before and after measurements to eliminate errors in concentration due to evaporation of solvent. Several concentrations were usually made from a single sample by dilution with filtered solvent, followed by a period of mixing and equilibration before further measurements.

A fourth order cumulant expansion was fitted to the field autocorrelation function to determine the mean initial decay rate $\bar{\Gamma}$ and normalized second moment of the distribution of decay rates $\mu_2/\bar{\Gamma}^2$ of the field autocorrelation function for each sample. Some samples exhibited large fluctuations in scattered intensity, indicating contamination by strongly scattering dust or gel-like particles. In these cases, the few affected runs were discarded. Measurements at scattering

Table 4
A comparison of the SANS experimental parameters from ANSTO and NIST

Parameter	ANSTO	NIST
Wavelength	3.5 Å	6.5 Å
$\Delta\lambda/\lambda$	15%	25%
Sample–detector distance	5 m	2.03 m
Detector offset	0°	7.5°
Flux	10^4 n cm^{-2} s^{-1}	10^{11} n cm^{-2} s^{-1}
Experimental q range	0.009 Å^{-1} $<q<$ 0.18 Å^{-1}	0.016 Å^{-1} $<q<$ 0.321 Å^{-1}

angles between 40 and 100° for a typical sample indicated that the diffusion coefficient obtained by this technique was independent of scattering vector. All measurements on other samples were made at a scattering angle of 50°.

The theory of dynamic light scattering from polymer solutions is discussed in several excellent books and reviews, e.g. [12–14]. The interpretation of dynamic light scattering from a solution of polymer in a good solvent at small scattering vector ($qR_g < 1, q = (4\pi n/\lambda)\sin(\theta/2)$) is straightforward. At infinite dilution, the mean decay rate is related to the zero concentration limit of the mutual diffusion coefficient of the polymer in the given solvent, $\bar{\Gamma}/q^2 = D_0$. Under these conditions, D_0 is equal to the self-diffusion coefficient of the polymer, and the hydrodynamic radius of the polymer can be obtained from the Stokes–Einstein equation as $R_h = k_B T/6\pi\eta_0 D_0$, where k_B is Boltzmann's constant and η_0 is the solvent viscosity. At higher concentrations that are still below the overlap concentration, the mean decay rate is related to the mutual diffusion coefficient, $\bar{\Gamma}/q^2 = D_m$, which has a concentration dependence that is well-described by a virial-type expansion, with $D_m = D_0(1 + k_D c + \cdots)$. In the semidilute region, a pseudo-gel response is predicted, due to the effect of temporary entanglements that become important above the overlap concentration, and the short-time diffusion coefficient obtained from the initial value of the mean decay rate is called the cooperative diffusion coefficient, $\bar{\Gamma}^2/q^2 = D_c$. For a polymer in a good solvent, D_c is dominated by the osmotic part, which is identical to the long-time mutual diffusion coefficient, and the field autocorrelation function is therefore expected to be well approximated by a single exponential decay [14]. We found this to be satisfied for all of our samples, with values of $\mu_2/\bar{\Gamma}^2$ typically <0.05 and always <0.10 for the results reported here.

De Gennes has derived a scaling law for the cooperative diffusion coefficient that is commonly used as an operational definition of the hydrodynamic screening length, ξ_h [15]. Thus, we used the definition

$$\xi_h = \frac{k_B T}{6\pi\eta_0 D_c} \tag{3}$$

to calculate the hydrodynamic screening length for semidilute solutions.

All DLS measurements were performed at a temperature of 25.0 ± 0.1 °C.

More detailed descriptions of the sample preparation procedures, data acquisition routines and data analysis methods for the SANS and DLS measurements are available elsewhere [9].

3. Results and discussion

3.1. Polystyrene solutions

We performed two sets of preliminary measurements on systems that have previously been studied by Brown and Mortensen [16], to validate our experimental and data analysis techniques, and provide data for comparison with the PDMS and PMMA solutions. The systems studied in the preliminary measurements were (d-) PS-THF and PS-DCM.

Our SANS measurements on the d-PS-THF solutions were the first quantitative measurements made using the ANSTO SANS facility, so a careful validation procedure was necessary. In all cases, our results agreed well with those of Brown and Mortensen [16]. The overlap concentration for this molar mass, estimated from

$$c^* = \frac{3M}{4\pi N_A R_g^3}, \tag{4}$$

using $R_g = 0.0160 M_w^{0.58\pm0.01}$ nm [28], is equal to 17.9 mg cm^{-3}. The static screening length for concentrations above the overlap concentration was found to vary with concentration as $\xi_s = 2.6c^{-0.67}$, which compares well with Brown and Mortensen's result $\xi_s = 2.2c^{-0.68}$ [16] for an almost identical molar mass, concentration range, and temperature.

The second set of preliminary measurements consisted of DLS measurements made on a PS-DCM system, once again almost identical to the one studied by Brown and Mortensen [16]. The value of c^* for this system, calculated using Eq. (4) and a value for R_g taken from Ref. [16] is again 17.9 mg cm^{-3}. This means that the concentrations studied extend from the dilute region up to $c/c^* \approx 7$. The limiting zero-concentration value of the diffusion coefficient, D_0, was found to be 4.96×10^{-11} m^2 s^{-1}, in good agreement with the value of 4.9×10^{-11} m^2 s^{-1} which can be read from Fig. 4 of Brown and Mortensen [16]. A plot superimposing our values for ξ_h in the semidilute region on Brown and Mortensen's shows good agreement between the two data sets. Note that for this comparison only, D_c was

divided by $(1-\phi)$, where ϕ is the polymer volume fraction, before calculating ξ_h using Eq. (3) so that our data analysis would be consistent with that of Brown and Mortensen [16]. It has been claimed that the theoretical result of de Gennes for the hydrodynamic screening length is calculated in the solvent fixed frame of reference, making the correction necessary to bring the experimental diffusion coefficients into the appropriate reference frame. However, this correction remains controversial and is often not applied. Furthermore, for semidilute solutions of sufficiently high molar mass, the volume fraction of polymer will become negligible, and the correction will become irrelevant. No other results reported in this paper have had this correction applied.

The concentration dependence of the hydrodynamic screening length of PS in several additional solvents with differing solvent quality was also studied. The results for the dilute and semidilute regions are summarised in Table 5. The low value of the infinite dilution diffusion coefficient for the PS-CCl_4 solution reflects the high viscosity of CCl_4 compared to that of the other solvents, and the lower value of k_D correlates with the poorer solvent quality of CCl_4, which should be regarded as a marginal, rather than good solvent for PS [17]. At concentrations above approximately 90 mg cm^{-3}, we find a decrease in the slope, and a departure from power law behaviour in D_c vs c for PS-CCl_4 solutions, due to a weakening of the thermodynamic factor and simultaneous increase in the frictional factor in the mutual diffusion coefficient. This agrees with the observations of Wang and Zhang [18].

All of the data for the concentration dependence of the hydrodynamic screening length ξ_h in PS-solvent solutions are shown in Fig. 1.

3.2. PMMA and PDMS solutions

Measurements of the static screening length ξ_s in PMMA and PDMS solutions were conducted using the ANSTO SANS and NIST small angle neutron scattering spectrometers, as described earlier. Some measurements were performed on both instruments as a test of the reproducibility of the experimental and data analysis procedures. Figs. 2 and 3 show that the results obtained on the two instruments using different samples agree within experimental uncertainties. Uncertainties in the ξ_s values were calculated from the uncertainties in the least squares values of the slope and intercept used to calculate each ξ_s value. The large uncertainties in the measurements performed at ANSTO using the ANSTO SANS instrument result from the far lower neutron flux (see Table 4). All SANS measurements on PDMS solutions were performed using the PDMS2 polymer (see Table 1). Details of the solutions studied are given in Table 3.

The collected static screening length results for all polymer–solvent pairs are shown in Fig. 4. The overlap concentrations calculated using Eq. (4) for the systems used in SANS measurements are: $c^*=21$(PMMA/d-Benz), 19 (PMMA/d-THF), 24 (PMMA/d-Tol), 29 (PDMS/d-Benz) and 31 (PDMS/d-Tol) mg cm^{-3}. No literature value of R_g was available for the PDMS/d-THF system, so we were unable to calculate a value of c^* for that solution. However, it is clear that almost all of the concentrations studied are above the overlap concentration. There is a large spread in the data collected for different polymer–solvent pairs, but each individual data set displays apparent power law behaviour above the overlap concentration. The values of the power law exponents are discussed in Section 3.3.

The hydrodynamic screening length ξ_h was measured for the PMMA and PDMS solutions described in Table 3. Some of the solutions that were studied by neutron scattering could not be studied with DLS because the scattering was too weak to give reliable results due to the small refractive index increment. The overlap concentrations for the solutions were calculated using Eq. (4) to be: 19 (PMMA/d-THF), 39 (PDMS/d-Benz) and 37 (PDMS/d-Tol) mg cm^{-3}. Note that DLS measurements were performed on both PMMA/d- THF and PMMA/THF solutions, giving identical results for the concentration dependence of the hydrodynamic screening length and dilute solution parameters. The results for the two systems are merged and presented together in Table 6. Fig. 5 shows the results for the concentration dependence of the hydrodynamic screening lengths.

Results for the infinite dilution dilution diffusion coefficient, hydrodynamic radius, linear concentration coefficient k_D, and the power-law fit to the cooperative diffusion coefficient for PMMA and PDMS solutions are summarized in Table 6.

3.3. Comparison with theory

Concentration power law exponents x for the static screening length in the semidilute region, defined by $\xi_s \propto c^x$, are shown in Table 7. The values of x range from -0.55 to

Table 5
DLS results for PS/solvent systems in the dilute and semidilute regions

Solution	D_0 (10^{-11} m^2/s)	R_h (nm)	k_D (cm^3/g)	D_c (10^{-11} m^2/s)
PS/THF	4.82	9.94	35.7	1.31 $c^{0.559}$
PS/Tol	3.97	9.82	33.8	1.69 $c^{0.449}$
PS/CCl_4	2.38	10.09	26.2	1.08 $c^{0.453}$
PS/DCM	4.96	10.66	33.7	1.41 $c^{0.577}$

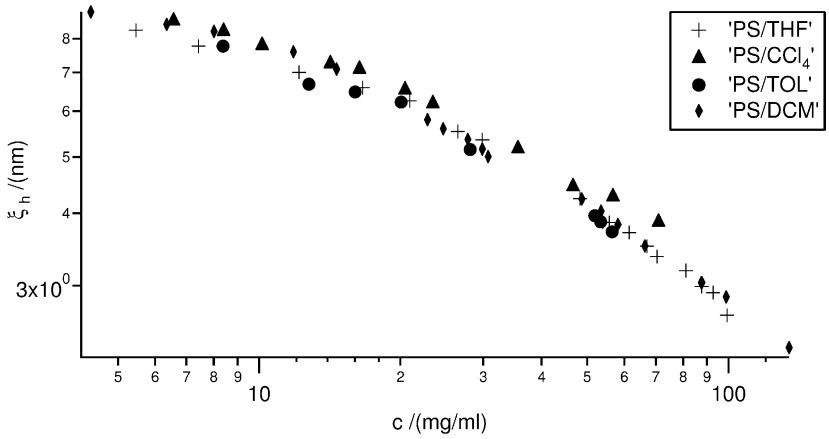

Fig. 1. ξ_h vs c for PS/solvent systems over the whole concentration range.

Table 6
DLS results for PMMA and PDMS solutions in the dilute and semidilute regions

Solution	D_0 (10^{-11} m^2/s)	R_h (nm)	k_D (cm^3/g)	D_c (10^{-11} m^2/s)
PMMA/d-THF	4.133	10.73	22.3	1.36 $c^{0.462}$
PDMS/d-Tol	4.318	8.72	17.31	1.45 $c^{0.433}$
PDMS/d-Benz	3.767	8.40	11.29	1.032 $c^{0.438}$

Table 7
Concentration exponents x for the static screening length in d-PS/THF, PMMA/d-solvent and PDMS/d-solvent systems

Solution	Concentration Exponent
d-PS/THF	−0.780
PDMS/d-Benz	−0.550
PDMS/d-THF	−0.590
PDMS/d-Tol	−0.552
PMMA/d-Benz	−0.770
PMMA/d-THF	−0.776
PMMA/d-Tol	−0.646

−0.78. The asymptotic theoretical value of this exponent for a polymer in a good solvent is $x = -\nu/(3\nu - 1)$, giving $x = -0.75$ if it is assumed that $\nu = 0.6$, or -0.77 if we take $\nu = 0.588$. The values of x displayed in Table 9 indicate that the asymptotic limit has only been reached for the d-PS/THF, PMMA/d-Benz and PMMA/d-THF solutions. The others are apparently affected by crossover effects.

The marginal solvent theory of Schaefer, Joanny and Pincus [20,21] offers a possible explanation for the low values obtained for these exponents. Marginal solvent theory takes into account the limited flexibility of real

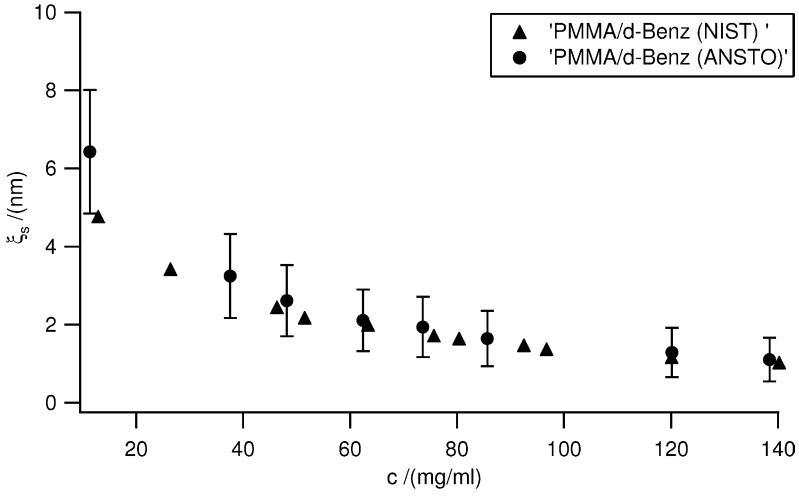

Fig. 2. A comparison of PMMA/d-Benz ξ_s vs c data from ANSTO and NIST.

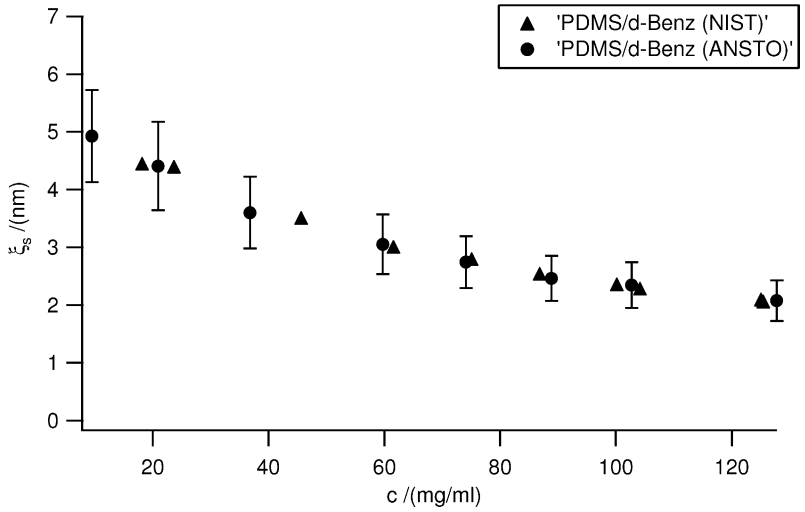

Fig. 3. A comparison of PDMS/d-Benz ξ_s vs c data from ANSTO and NIST.

polymer chains and postulates the existence of a semidilute marginal regime, between the semidilute good solvent regime and the semidilute theta regime or the concentrated regime. For a given polymer–solvent combination, the crossover from the semidilute good solvent regime to the semidilute marginal regime occurs at a constant value of the volume fraction $\tilde{\phi}$, regardless of the molar mass. The crossover concentration from the dilute to the semidilute good solvent regime, however, increases as the molar mass decreases. Therefore, the semidilute good solvent regime becomes narrower as the molar mass decreases, disappearing completely if the molar mass is decreased sufficiently. Marginal solvent theory predicts that the concentration exponent of the static screening length should be -0.5 in the semidilute marginal region. When each polymer–solvent pair is considered separately and only a few molar masses are studied, this explanation for the low values of ξ_s appears plausible. However, Brown and Nicolai have remarked that marginal solvent theory does not adequately describe their large data collection. In fact, they remarked that semidilute good solvent scaling behaviour is observed up to concentrations approaching 30% for solutions of polystyrene in good solvents, well beyond the expected crossover to the concentrated regime.

A simple plot of $\log(\xi_s)$ vs $\log(c)$ for only one molar mass does not give a true indication of whether the asymptotic region has been reached, because apparent power-law behaviour is observed even for solutions in the crossover from dilute to semidilute behaviour. Therefore, it is more informative to plot data obtained for several different molar masses against $\log(c)$ and use the onset of molar mass independence as an indication of asymptotic behaviour. This is a fruitful approach when a single polymer–solvent combination is studied. However, this method does not account for differences in solvent quality. A better approach, suggested by renormalization-group theory, is to plot the

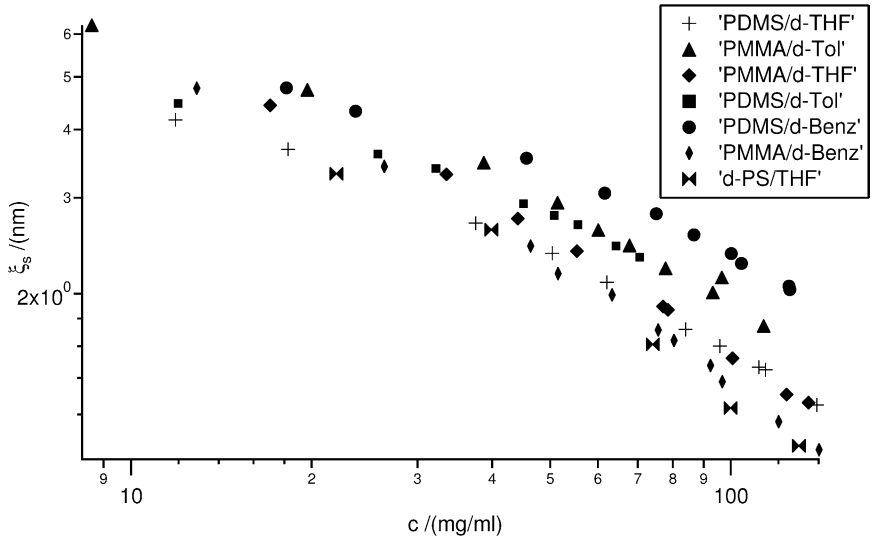

Fig. 4. ξ_s vs c for all polymer/solvent systems.

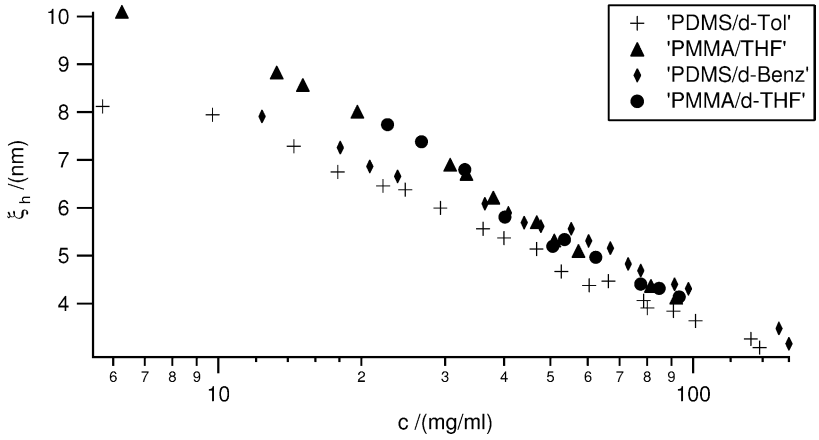

Fig. 5. ξ_h vs c for PMMA/solvent and PDMS/solvent systems.

normalized screening length, ξ_s/R_g against the reduced concentration or overlap parameter $X = 16/9A_2M_wc$. In the long-chain limit, this reduction should remove both molar mass and solvent quality differences, producing a universal plot. Wiltzius et al. [19] have confirmed that a universal plot is obtained when data for various molar mass polystyrenes in solutions with differing solvent quality were plotted in this way. Brown and Nicolai [6] have subsequently shown that almost all of the known data for the static screening length in polystyrene-good solvent solutions available up to 1990 can be reduced to a universal plot. The question that now arises is whether solutions of polymers with different backbone flexibility characteristics from polystyrene also fall on a universal curve when plotted in this way. Fig. 6 shows a plot of $\xi_s = R_g$ against $X = 16/9A_2M_wc$ for all of the solutions studied in this work. Comparing this with Fig. 4, we see a remarkable collapse of the data onto a narrow band. This reduction requires knowledge of the dilute-solution properties R_g and A_2, which we were unable to measure. We were therefore forced to either use published values or estimated values of these quantities. The sources of our values of these quantities are summarised in Table 8. The values of R_g for the PDMS/Benz and PMMA/Tol systems were estimated using the Flory Fox relation. The remaining systematic deviations in Fig. 6 are probably due to poor estimation of the values of the second virial coefficients, A_2 for the PDMS/d-THF and PDMS/d-Benz solutions, for which we were unable to find literature values.

Table 8
Sources for R_g and A_2 values

Polymer	R_g	A_2
PMMA/Benz	[22]	[23]
PDMS/Benz	Flory-Fox	From PMMA/Benz
PMMA/Tol	Flory-Fox	[24]
PDMS/Tol	[26]	[25]
PMMA/THF	[27]	From PMMA/Benz
PDMS/THF	From PDMS/Tol	From PDMS/Tol
PS/THF	[28]	[29]

A similar plot of the scaled hydrodynamic screening length ξ_h/R_h against $X = 16/9A_2M_wc$ is shown in Fig. 7. This scaling is clearly not sufficient to reduce all of our data for the hydrodynamic screening length to a single universal curve. However, this is not surprising, because our dynamic

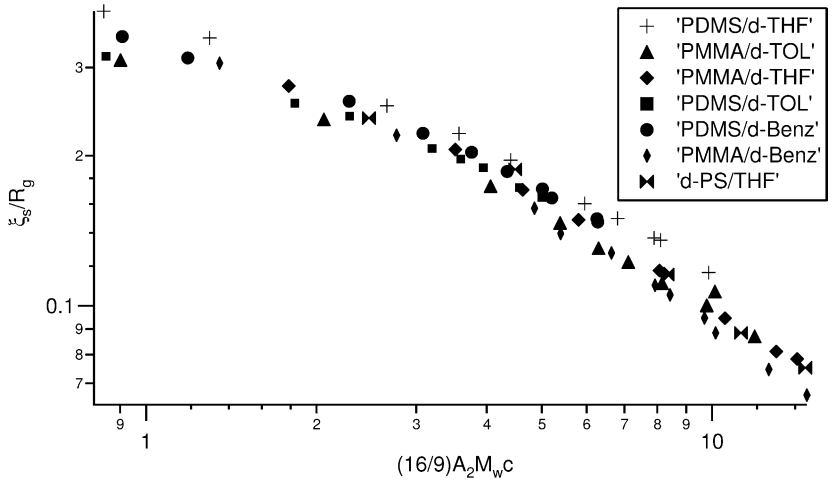

Fig. 6. ξ_s/R_g vs $(16/9)M_wA_2c$ for all polymer/solvent systems.

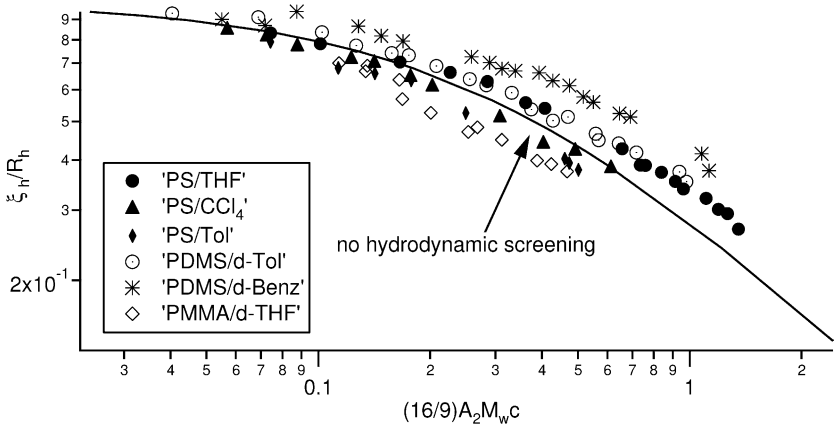

Fig. 7. ξ_h/R_h vs $(16/9)A_2M_wc$ for PS/solvent, PMMA/solvent and PDMS/solvent systems. The curve is Shiwa's form for ξ_h/R_h vs X in the absence of hydrodynamic screening [30].

light scattering measurements were restricted to rather low values of X. A universal curve would only be expected at values of X greater than 1. What is surprising in Fig. 7 is that there does not seem to be any tendency towards universality as X approaches and exceeds 1. It appears that substantially higher values of X are required for universal behaviour of ξ_h/R_h than for universal behaviour of ξ_s/R_g. This has also been found by Wiltzius et al. [31], who studied the concentration dependence of the hydrodynamic screening length of solutions of polystyrene in various solvents. Following Wiltzius et al. [31], we have also plotted ξ_h/R_h against k_Dc, where k_D is the coefficient of the linear term in the concentration dependence of the mutual or cooperative diffusion coefficient. The result, shown in Fig. 8, is an apparently universal curve, with a relatively simple dependence on k_Dc, extending to concentrations far higher than those for which a simple linear relation between D_c and c holds.

It is also of interest to investigate the concentration dependence of the ratio of hydrodynamic to static screening lengths. The concentration dependence of the static and hydrodynamic screening lengths for the four systems for which we have measured both quantities is shown in Table 9. The exponents for ξ_s are consistently higher, and closer to the asymptotic values than the exponents for ξ_h. This clearly occurs because our concentrations and molar masses are too low for the asymptotic limit to be reached, especially for the hydrodynamic screening lengths. The final column in Table 9 shows the concentration exponent z of ξ_h/ξ_s. For all of the systems studied, the value of z is positive, and similar in value, except for the value for the PMMA/d-THF system, which is far larger. This is a consequence of the fact that the exponent for ξ_s is remarkably close to the asymptotic limit, while the exponent for ξ_h is still far from the asymptotic value. This confirms again that the asymptotic limit is far more rapidly approached for the static properties than for the hydrodynamic properties.

Table 9
Concentration relationships for ξ_s and ξ_h used to calculate ratios

Solution	Relationship for ξ_h	Relationship for ξ_s	z
PS/THF	$36.39\ c^{-0.559}$	$26.16\ c^{-0.670}$	0.111
PDMS/d-Tol	$24.60\ c^{-0.433}$	$29.50\ c^{-0.552}$	0.119
PDMS/d-Benz	$30.65\ c^{-0.438}$	$29.50\ c^{-0.550}$	0.112
PMMA/d-THF	$31.61\ c^{-0.468}$	$55.50\ c^{-0.776}$	0.308

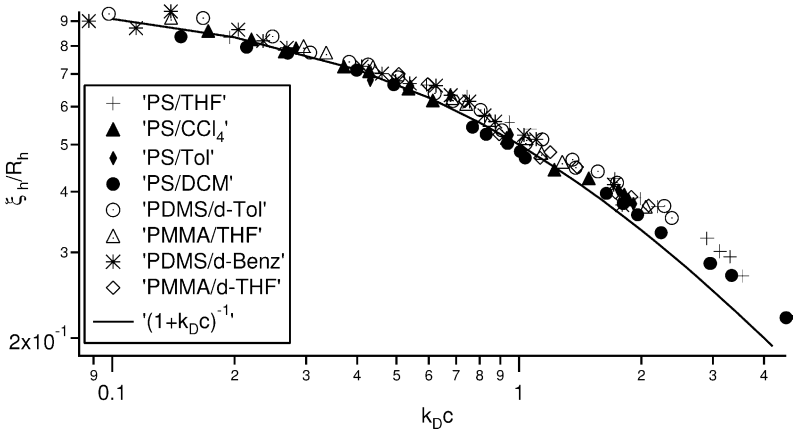

Fig. 8. ξ_h/R_h vs k_Dc for PS/solvent, PMMA/solvent and PDMS/solvent systems. The solid line shows the function $(1+k_Dc)^{-1}$.

4. Conclusion

We have measured the static and hydrodynamic screening lengths of polystyrene, polymethylmethacrylate and polydimethylsiloxane in a variety of solvents using small angle neutron scattering and dynamic light scattering. Some of the neutron scattering results were made on a new small angle neutron scattering spectrometer at the Australian Nuclear Science and Technology Organization. The results obtained from this spectrometer agreed well with those measured independently at the Center for Neutron Research, NIST, Gaithersburg, validating the spectrometer operation and data reduction and analysis procedures for the new spectrometer.

The concentration dependence of the scaled static screening length ξ_s/R_g follows a universal curve when plotted as a function of the overlap parameter, $X=(16/9)M_wA_2c$, at values of X greater than 1. This is in agreement with previous results, which have almost exclusively been obtained from solutions of polystyrene in various solvents, and it confirms that the static properties are independent of the details of the polymer and solvent interactions. Our results for the hydrodynamic screening length are less conclusive, for several reasons. When we plotted the scaled hydrodynamic screening length ξ_h/R_h against X, we found that the data were scattered and showed no sign of converging at values of X greater than 1. However, we were unable to study the behaviour of ξ_h/R_h at values of X much greater than 1, mainly due to the low molar masses of our samples. When we plotted our values of ξ_h/R_h against k_Dc, a universal curve was obtained up to $k_Dc=4$. This is probably due to the relatively weak departure of the cooperative diffusion coefficient from linear concentration dependence in the concentration and molar mass range studied. One of the consequences of the non-asymptotic behaviour of ξ_h/R_h that we observe is that the ratio of the hydrodynamic to static screening length is concentration dependent. We find that the difference between the two exponents is greatest for the PMMA/d-THF system, probably because this system has already reached the asymptotic behaviour for ξ_s, while the behaviour of ξ_h remains far from asymptotic.

We hope that these results will prompt further work, using higher molar masses, to investigate the behaviour of the static and hydrodynamic screening lengths for a diverse variety of polymer–solvent pairs, to complement the data presented here and the previously published data which has mainly been measured for polystyrene–solvent systems.

Acknowledgements

This work was supported by the Cooperative Research Centre for Polymers and AINSE. We would like to thank Bill van Megen, Gary Bryant and Phil Francis for their expert advice on the DLS experiments. We acknowledge the support of the National Institute of Standards and Technology, U.S. Department of Commerce, in providing the neutron research facilities used in this work.

References

[1] de Gennes P-G. Scaling concepts in polymer physics. Ithaca: Cornell University Press; 1979.
[2] des Cloizeaux J, Jannink G. Polymers in solution: their modelling and structure. Oxford: Clarendon Press; 1990.
[3] Doi M, Edwards SF. The theory of polymer dynamics. Oxford: Clarendon Press; 1986.
[4] Oono Y. Adv Chem Phys 1985;61:301.
[5] Daoud M, Jannink G. J Phys (Paris) 1976;37:973.
[6] Brown W, Nicolai T. Colloid Polym Sci 1990;268:977.
[7] Daoud M, Cotton JP, Farnoux B, Jannink G, Sarma G, Benoit H, Duplessix R, Picot C, de Gennes PG. Macromolecules 1975;8:804.
[8] Hammouda B, Krueger S, Glinka CJ. J Res Natl Inst Stand Technol 1993;98:31.
[9] Bennett A., MAppSc Thesis, RMIT University: Melbourne, Australia, 2003.
[10] Higgins JS, Benoit HC. Polymers and neutron scattering. Oxford: Clarendon Press; 1996.
[11] Segre PN, van Megen W, Pusey PN, Schatzel K, Peters W. J Mod Opt 1995;42:1929.
[12] Berne B, Pecora R. Dynamic light scattering. New York: Wiley; 1976.
[13] Brown W, editor. Dynamic light scattering: the method and some applications. Oxford: Clarendon Press; 1993.
[14] Wang CH. In: Brown W, editor. Dynamic light scattering: the method and some applications. Oxford: Clarendon Press; 1993.
[15] de Gennes PG. Macromolecules 1976;9:594.
[16] Brown W, Mortensen K. Macromolecules 1988;21:420.
[17] Park S, Chang T, Lee JW, Pak H. Bull Korean Chem Soc 1991;12:682.
[18] Wang CH, Zhang XQ. Macromolecules 1995;28:2288.
[19] Wiltzius P, Haller HR, Cannell DS, Schaefer DW. Phys Rev Lett 1983;51:1183.
[20] Schaefer DW, Joanny JF, Pincus P. Macromolecules 1980;13:1280.
[21] Schaefer DW. Polymer 1984;25:387.
[22] Kok C, Rudin A. J Appl Polym Sci 1981;26:3583.
[23] Numasawa N, Kuwamoto K, Nose T. Macromolecules 1986;19:2593.
[24] Fox TG, Kinsinger JB, Mason HF, Schuele EM. Polymer 1962;3:71.
[25] Anasagasti M, Katime I, Strazielle C. Macromol Chem Phys 1987; 188:201.
[26] Ould Kaddour L, Strazielle C. Polymer 1987;28:459.
[27] Jackson C, Chen Y, Mays JW. J Appl Polym Sci 1996;61:865.
[28] Park S, Chang T, Lee JW, Pak H. Bull Korean Chem Soc 1991;12:682.
[29] Venkataswamy K, Jamieson AM, Petschek RG. Macromolecules 1986;19:124.
[30] Shiwa Y. Phys Rev Lett 1987;58:2102.
[31] Wiltzius P, Haller HR, Cannell DS, Schaefer DW. Phys Rev Lett 1984;53:834.